Senior Thesis

Differentiation Mechanisms in a Calc-alkaline Lava Series from the Island of Aegina, Aegean Sea, Greece

by

Kenneth S. Johnson
1987

Submitted as partial fulfillment of
the requirements for the degree of
Bachelor of Science in Geology and
Mineralogy at the Ohio State University,
Autumn Quarter, 1987

Approved by:

M. Barton

Dr. Michael Barton

TABLE OF CONTENTS

ABSTRACT

Major and trace element and isotopic modelling was performed on four representative lava samples from the island of Aegina, Aegean Sea, using data obtained from Barton et al. (1985). Aegina is situated on the western-most end of the Hellenic volcanic arc, in which one continental plate is being subducted beneath another. Major oxide variations suggest differentiation largely via fractional crystallization, and mixing models support this theory. 87Sr/86Sr behavior lends evidence to the probability of assimilation, most prominent in the early stages of differentiation. Failure to predict the effects of combined assimilation and fractional crystallization suggests the use of inaccurate values of Sr(ppm) and 87Sr/86Sr for the crust. However, the results presented provide useful information for the interpretation of destructional plate environments.

TABLES AND FIGURES

LIST OF TABLES

LIST OF FIGURES

1.0 INTRODUCTION AND PURPOSE OF THE STUDY

The volcanism of the Aegean Sea is controlled by destructional plate margins, that is, one continental plate being subducted, or pushed, beneath another. According to Ringwood (1974), this subduction results in the dehydration of the subducted slab and partial melting of both the slab and the overlying upper mantle. The liquid generated by this process migrates upward and comes to rest in an intra-crustal magma chamber. There the magma is subjected to one or more different processes (i.e. fractional crystallization, magma mixing, and assimilation) that greatly alter its geochemical characteristics before it is erupted onto the surface.

Brief definitions of the three most common processes are necessary. Fractional crystallization is the removal of early-formed phases and the subsequent depletion of the involved elements in the liquid. Assimilation is the incorporation of crustal material into the melt. Finally, magma mixing, as the name implies, is the mixing of two liquids of differing compositions. It is these three processes that we attempt to determine.

The lavas from Aegina are calc-alkaline in nature, ranging from basaltic andesite to rhyodacite. Available studies of the volcanics of Aegina appear limited to the investigation of the major oxides alone (Till, 1986). Un-

fortunately, these oxides are not very sensitive indicators of magmatic processes. Trace elements and Sr isotopes, however, place much better constraints on intra-crustal processes. As Barton (1986) states, one must recognize the processes that occur in shallow magma chambers before any conclusions can be drawn as to the nature of the upper mantle. The purpose of this study is to determine the processes involved in the evolution of the lavas found on the island of Aegina.

The approach to this problem focusses attention on four lava samples from Aegina (Aeg 3, Aeg 14, Aeg 13, and Aeg 17) which represent different stages in a continuous calc-alkaline series, including the two end-members. Complete major oxide and trace element models of these samples are presented, and are also incorporated with those of the remaining samples in the variation diagrams to get a better overall view of the behavior of this series.

2.0 SUMMARY

Results of this study, and of others (Till, 1986), suggest that these lavas are related largely via fractional crystallization that operated throughout the differentiation of the lava series. However, some evidence (e.g. 87Sr/86Sr variations) points to the workings of assimilation, probably of lower crustal material due to the relative ease of incorporating already-heated rocks into the liquid. Evidence for magma mixing is simply not substantial. However, more detailed studies must be conducted before any conclusions as to the possibilities of mixing can be established.

3.0 GEOLOGIC SETTING

The island of Aegina is located at the western end of the Hellenic volcanic arc, just off the Greek Mainland (see Fig. 1.). This volcanic arc is the result of continental-continental or continental-subcontinental interactions related to the subduction of the African plate beneath the Aegean microplate, which began about 12 million years ago. Active volcanism along this arc, however, dates back only to about 3 million years ago (Fytikas et al., 1976).

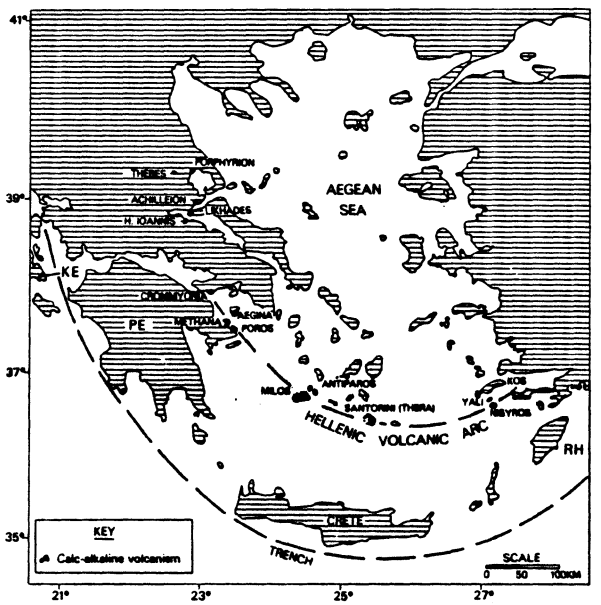

Fig. 1. The Hellenic volcanic arc located in the Aegean Sea.

It is believed that there is a double arc structure which may explain recent volcanic activity. According to this theory, the outer arc contains the islands of Crommyonia, Methana, Aegina, Poros, Milos, Santorini, Yali, and Nisyros. The inner arc includes Porphyrion, Thebes, Achilleion, Likhades, Hagios Ioannis, Antiparos, and prob-

ably Kos (Huijsmans, 1985).

Volcanism along this arc is predominantly calc-alkaline in nature, with some alkaline volcanism occurring on a few islands (e.g. Patmos and Lesvos) (Fytikas et al., 1976). The last volcanic eruption in this area was in 1950 on the island of Santorini (Wyers and Barton, 1986).

4.0 METHODS

All samples were analyzed for major and trace elements by XRF at the Institute of Earth Sciences, Utrecht (The Netherlands), and by INAA and wet chemical methods at IRI, Delft. $^{87}Sr/^{86}Sr$ values were measured at the ZWO Laboratory for Isotope Geology, Amsterdam. Analyses were completed by M. Barton and G.P. Wyers.

Computer modelling and petrographic analyses were carried out at the Ohio State University, Columbus. Variation diagrams were completed on the plotter in the Hydrogeology Laboratory (OSU) with the help of Rodney Sheets.

5.0 RESULTS AND DISCUSSION

5.1 PETROGRAPHY

Petrographic studies were performed on each of the samples, with those of the four representative lavas described below. All analyses were done on a Leitz polarizing microscope. As Till (1986) notes, all the samples exhibit a holocrystalline texture, with the more evolved lavas showing a slightly hypocrystalline nature. This is confirmed by the author. The common phenocryst phases include plagioclase, olivine, clinopyroxene, orthopyroxene, amphibole, and opaques (magnetite?). Oscillatory zoning in the plagioclase phenocrysts is common and, in the presence of hydrous phases (i.e. hornblende and biotite), attests to the role of water in the evolution of these magmas (Ringwood, 1974). The complex zoning makes it difficult for precise plagioclase compositions to be determined.

5.1.1. Basaltic andesite (Aeg 3).

Plagioclase (labradorite) is the dominant phase, making up approximately 80% of the rock. Zoning (normal, with some oscillatory) and complex twinning are common. The interiors of some of the phenocrysts are partially resorbed. Olivine (forsterite) is subhedral to euhedral and displays the characteristic irregular

system of cracks. It is found in small amounts as phenocrysts and in the groundmass. Slight alteration by iddingsite is common. Clinopyroxene (augite) is a minor phase and is found as subhedral to anhedral grains. Opaques are common and found largely as inclusions in the ultra-mafic minerals (i.e. olivine and clinopyroxene).

5.1.2. Andesite (Aeg 14).

Plagioclase (andesine to labradorite) is found as euhedral to subhedral phenocrysts, commonly displaying oscillatory zoning and complex twinning. Most grains exhibit at least partial resorption. Clinopyroxene (augite) and orthopyroxene grains are small and are generally euhedral to subhedral. Olivine is found in small amounts as euhedral to anhedral grains. Some are extensively resorbed and commonly display iddingsite rims. Amphibole (hornblende) is found as euhedral phenocrysts. It is commonly resorbed and pseudomorphic and contains inclusions of feldspar and opaques. Biotite, calcite (rimming vescicles), and opaques (as inclusions in ultra-mafic minerals) are found in lesser amounts.

5.1.3. Dacite (Aeg 13).

Plagioclase (oligoclase to andesine) is extensively zoned (oscillatory) and displays combined Carlsbad-albite twinning. Approximately half of the pheno-

crysts show partial to extensive resorption. Hornblende is commonly found as euhedral pseudomorphs. More birefringent grains exhibit zoning and simple twinning. Quartz is found in small amounts as rounded grains and is distinguished from the feldspars by its uniaxial positive character and complete lack of zoning. Clinopyroxene is found largely in the groundmass. Biotite, opaques, and trace amounts of apatite (as inclusions in the feldspars) are also found.

5.1.4. Rhyodacite (Aeg 17).

Plagioclase (oligoclase) and alkali feldspar are both commonly resorbed along the edges, and display oscillatory and normal zoning. However, the plagioclase is twinned, whereas the alkali feldspar is not. Hornblende is the dominant phenocryst phase with euhedral to subhedral forms. Some are glomeroporphyritic in nature. Clinopyroxene (in the groundmass), quartz, and opaques (concentrated in the hornblende phenocrysts) are found in small amounts.

5.2 WHOLE-ROCK CHEMICAL ANALYSES

In order to better understand the processes involved in the differentiation of this lava series, the entire evolution of these magmas has been defined by differentiation "steps", involving the four representative samples (i.e. Aeg 3, 14, 13, 17). Making the assumption that each lava is a derivative of the one listed before it, we consider Aeg 3 to be the most primitive (or undifferentiated) of the samples obtained, and Aeg 17 to be the most evolved (or differentiated). Therefore, in the following text, we say that the step Aeg 3 - 14 is the initial step, Aeg 14 - 13 the intermediate step, and Aeg 13 - 17 the latter step.

5.2.1 MAJOR ELEMENT RESULTS

As mentioned previously, the lavas from Aegina represent a continuous series from basaltic andesite to rhyodacite, with SiO2 concentrations ranging from about 55 to 70%, which is believed to reflect differentiation largely by fractional crystallization. The calc-alkaline nature of these rocks can best be illustrated in the simple AFM diagram in Fig. 2. The boundary line separates the tholeiitic field, in the upper portion, from the calc-alkaline field. Note the nearly complete lack of Iron enrichment, characteristic of a calc-alkaline suite. The chemical composi-

tions of the four representative lava samples are listed in full in Table I.

To better illustrate the variations of the major oxides during evolution, Harker diagrams are shown in Fig. 3. Note that SiO2 has been chosen as the differentiation index, due to its greater enrichment relative to the other elements. The major oxides behave just as expected for fractional crystallization. MnO exhibits a slight decrease while the other compatible elements (those that readily enter a crystal structure, i.e. CaO, Al2O3, MgO, TiO2, and FeO) show a marked decrease with increasing SiO2. A large amount of scatter appears in the Al2O3 plot, but the values for the representative lavas follow a straighter line. This scatter may, in part, be due to the porphyritic nature of the lavas (Huijsmans, 1985). The more incompatible elements

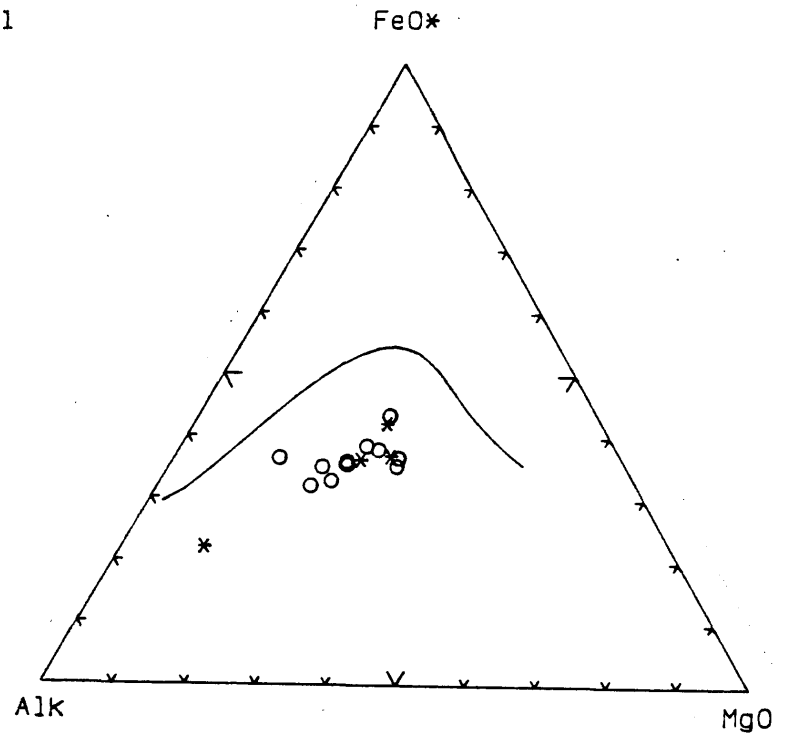

Fig. 2. AFM diagram. Note the relative lack of Iron enrichment in the calc-alkaline samples.

Table I. Chemical Compositions of the 4 Representative Lava Samples. (Aeg 3 - basaltic andesite, Aeg 14 - andesite, Aeg 13 - dacite, Aeg 17 - rhyodacite)

	Aeg 3	Aeg 14	Aeg 13	Aeg 17
SiO2	55.76	57.70	60.96	69.40
TiO2	0.77	0.61	0.51	0.30
Al2O3	17.57	17.29	16.57	15.62
FeO	7.03	5.87	5.23	2.40
MnO	0.16	0.16	0.14	0.09
MgO	4.53	4.84	3.82	1.24
CaO	9.07	8.32	7.40	3.76
Na2O	3.37	3.21	3.14	3.67
K2O	1.74	1.99	2.23	3.52
87Sr/86Sr	0.70415	0.70595	0.70594	0.70639
Sc	27.29	25.76	20.70	6.832
V	227.39	198.49	137.29	62.42
Cr	30.45	143.89	88.10	-
Zn	48.6	46.4	39.3	32.7
Rb	36.3	74.6	81.0	154.6
Sr	658.0	318.2	417.2	312.8
Y	18.1	18.1	17.8	17.4
Zr	143.1	98.0	110.9	112.5
Nb	1.2	3.8	4.7	10.3
Cs	1.54	3.71	3.54	10.89
Ba	296.0	467.0	684.0	592.0
La	18.31	17.54	19.35	33.48
Ce	32.64	30.41	33.71	47.83
Sm	3.94	2.894	2.88	3.62
Eu	0.966	0.955	0.822	0.805
Tb	0.505	0.96	0.504	0.446
Yb	1.55	1.74	1.23	1.802
Lu	0.262	0.366	0.276	0.240
Hf	2.975	2.690	2.29	3.236
Ta	0.49	-	0.553	-
Th	6.51	8.50	9.450	19.29
U	2.96	3.25	2.65	8.55

(i.e. K2O and Na2O), however, display an increase with increasing SiO2.

To determine if it is possible that these lavas could be related via fractional crystallization, a least squares mixing model (after Bryan et al., 1969) was constructed for

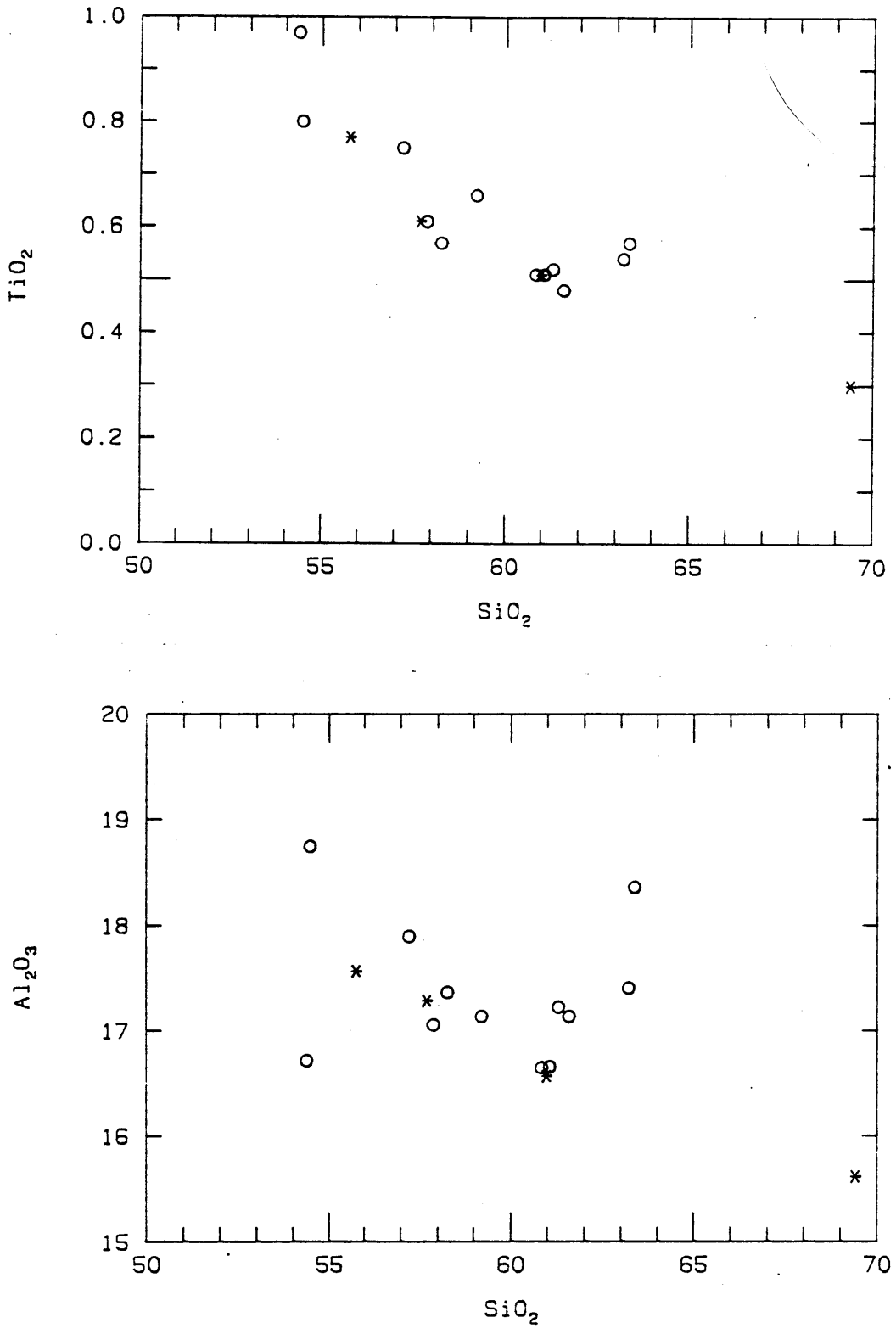

Fig. 3. Variation diagrams for the major oxides vs. SiO2.
* - representative sample

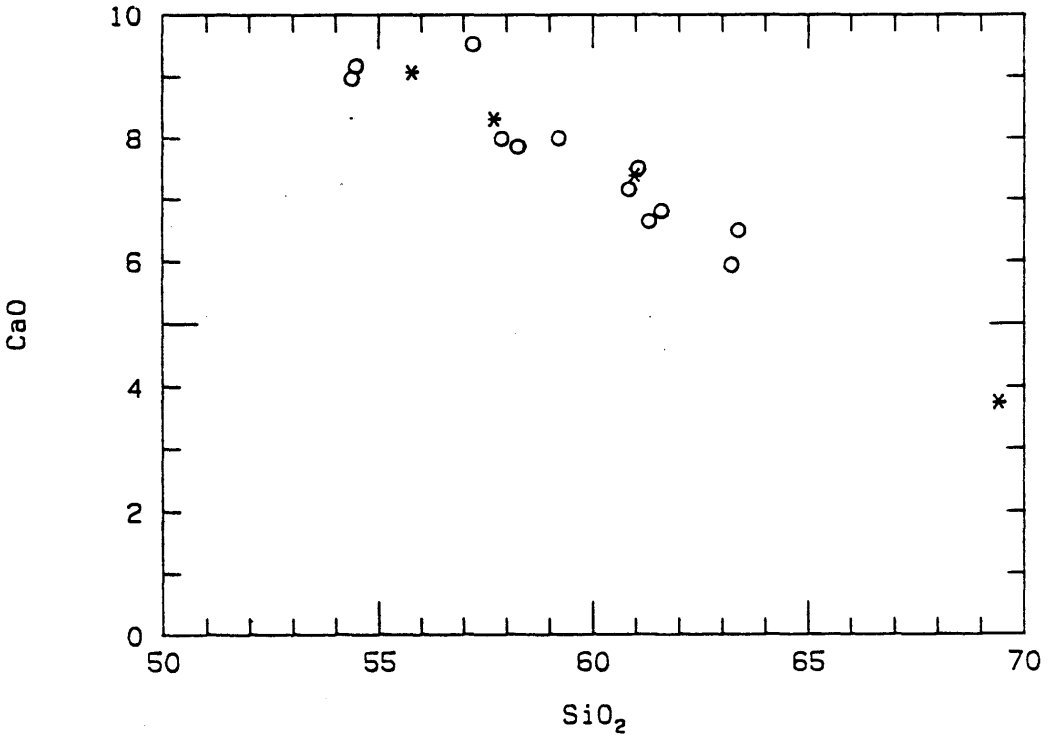
10
8
6
4
2
0
CaO
50
55
60
65
70
SiO2

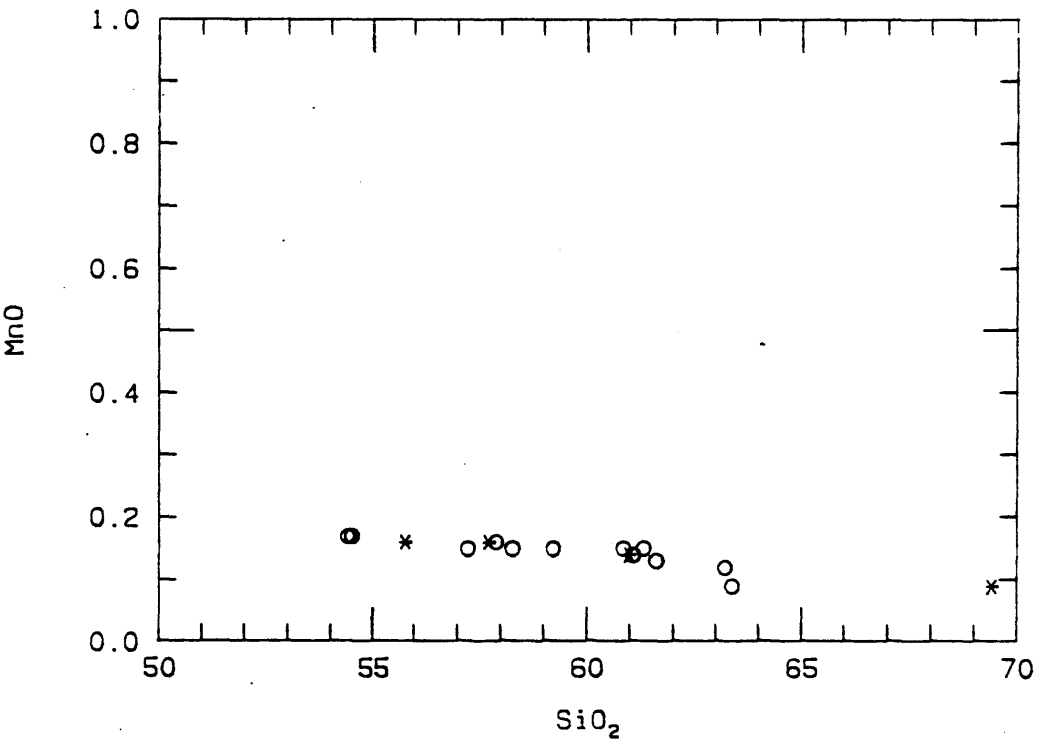
1.0
0.8
0.6
0.4
0.2
0.0
MnO
50
55
60
65
70
SiO2

Fig. 3. (cont.)

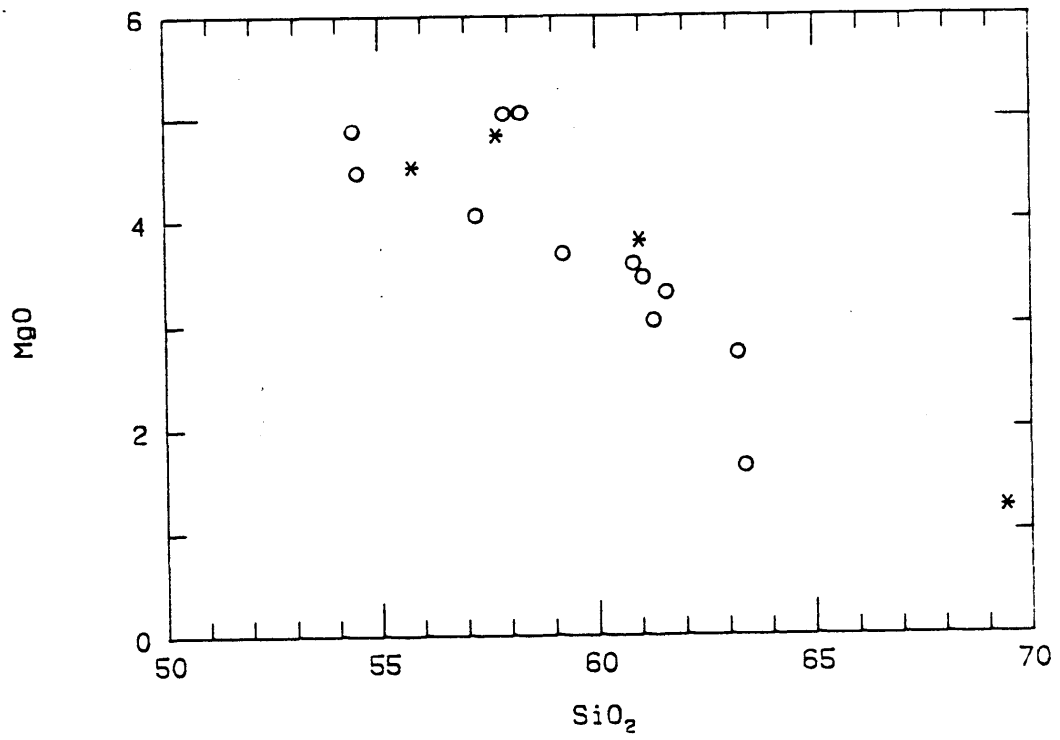

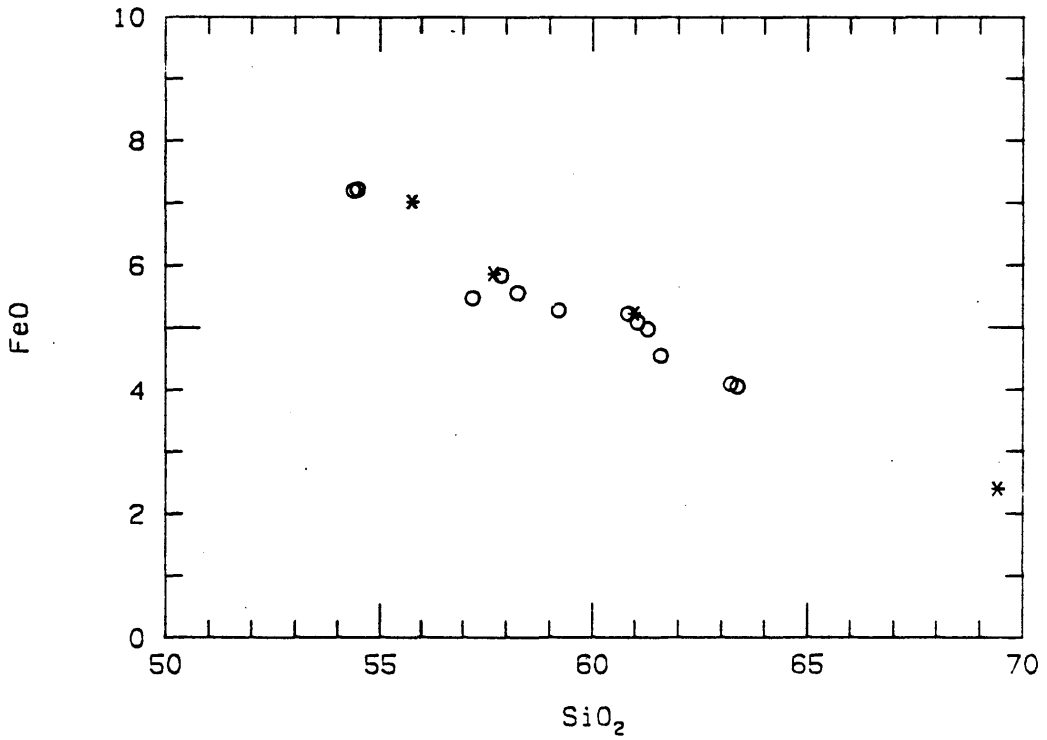

Fig. 3. (cont.)

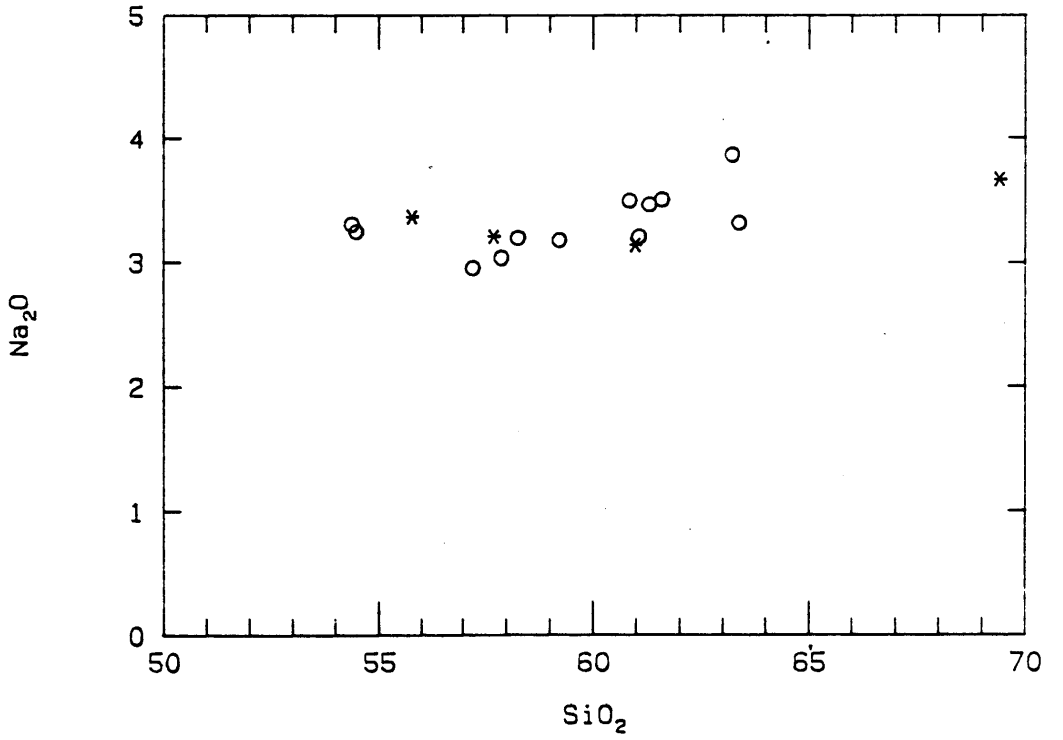

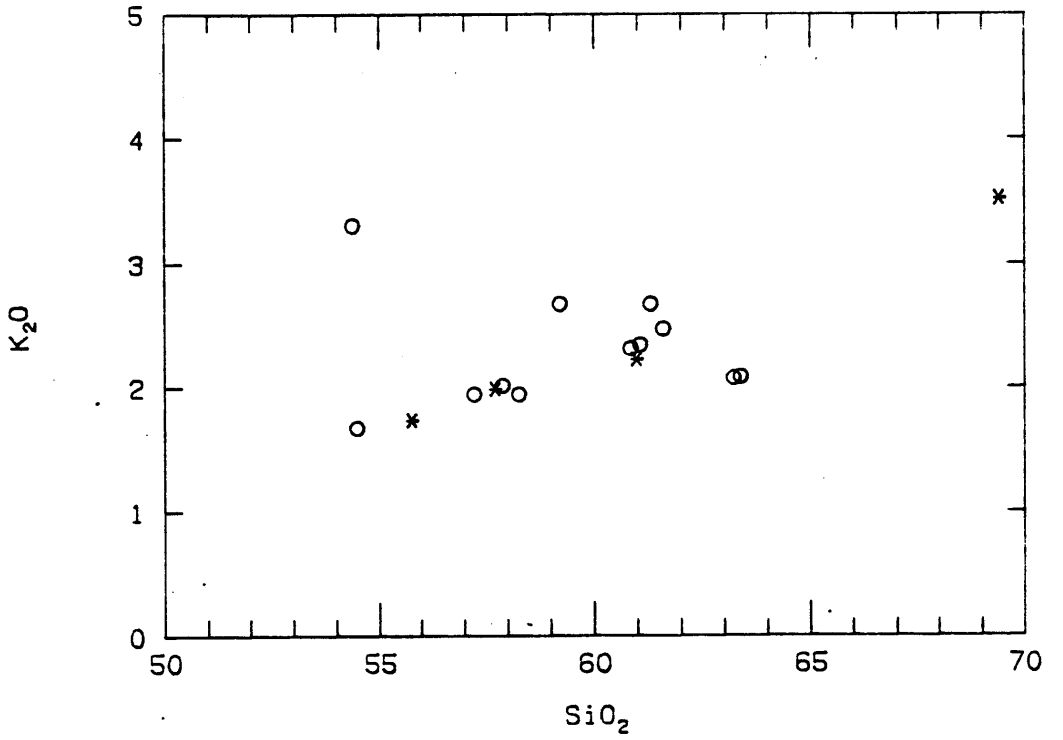

Fig. 3. (cont.)

each differentiation step, using the major oxide values from Table I. It is believed that, using this model, the crystallized phases (i.e. olivine, clinopyroxene, plagioclase, and magnetite) can be added back to the chemical composition of the daughter magma to produce a liquid with the composition of the parent magma.

The results of this model are presented in Table II.

Table II. Least Squares Mixing Model Results.

daughter Aeg 14 — parent Aeg 3

		obs.	est.	resid.
57.70	SiO2	55.76	55.75	0.0072
0.61	TiO2	0.77	0.77	0.0014
17.29	Al2O3	17.57	17.67	-0.1018
5.87	FeO	7.03	7.03	0.0083
0.16	MnO	0.16	0.15	0.0067
4.84	MgO	4.53	4.73	-0.1969
8.32	CaO	9.07	8.93	0.1400
3.21	Na2O	3.37	3.01	0.3648
1.99	K2O	1.74	1.78	-0.0472

*ssr: 0.2042

Aeg 14:	F	0.8942
	Ol	-
	Cpx	0.0198
	Plag	0.0649
	Op	0.0193
recalc. to 100%		
	Ol	-
	Cpx	0.1904
	Plag	0.6240
	Op	0.1856

daughter Aeg 17 — parent Aeg 13

		obs.	est.	resid.
69.40	SiO2	60.96	60.96	-0.0032
0.30	TiO2	0.51	0.39	0.1159
15.62	Al2O3	16.57	16.58	-0.0061
2.40	FeO	5.23	5.24	-0.0083
0.09	MnO	0.14	0.08	0.0603
1.24	MgO	3.82	3.82	0.0049
3.76	CaO	7.40	7.40	0.0044
3.67	Na2O	3.14	3.05	0.0875
3.52	K2O	2.23	2.24	-0.0136

*ssr: 0.0251

Aeg 17:	F	0.6279
	Ol	0.0256
	Cpx	0.0885
	Plag	0.2248
	Op	0.0308
recalc. to 100%		
	Ol	0.0692
	Cpx	0.2394
	Plag	0.6081
	Op	0.0833

daughter Aeg 13 — parent Aeg 14

		obs.	est.	resid.
60.95	SiO2	57.70	57.73	-0.0279
0.51	TiO2	0.61	0.48	0.1333
16.57	Al2O3	17.29	17.30	-0.0056
5.23	FeO	5.87	5.88	-0.0074
0.14	MnO	0.16	0.13	0.0343
3.82	MgO	4.84	4.81	0.0263
7.40	CaO	8.32	8.28	0.0436
3.14	Na2O	3.21	2.90	0.3081
2.23	K2O	1.99	1.83	0.1649

*ssr: 0.1445

Aeg 13:	F	0.8092
	Ol	0.0285
	Cpx	0.0219
	Plag	0.1218
	Op	0.0119
recalc. to 100%		
	Ol	0.1548
	Cpx	0.1190
	Plag	0.6616
	Op	0.0646

* sum of the squares of the residuals.

The residual column is simply the difference between the calculated and observed values of each oxide. The sum of the squares of the residuals (ssr) is a numerical expression of "misfits" and values of less than one (1) are considered an excellent fit (Huijsmans, 1985). From these results, it is clear that it is, indeed, possible that the members of this series are related by fractional crystallization. Unfortunately, however, the major oxides are not considered ideal indicators of other magmatic processes. Therefore, variations in trace element and Sr isotope values must be taken into account.

5.2.2 TRACE ELEMENT SYSTEMATICS

Trace elements are commonly used to determine the mechanisms of differentiation in magma bodies. The trace element contents of the representative lavas are listed back in Table I. The trace elements have also been plotted against SiO2 in Fig. 4. The data for Ba, Cr, and Ta have not been plotted, due to analytical error. There is simply too much scatter in the diagrams of Y, Tb, Sm, and Zr to get a clear idea of their behavior, probably again due to analytical uncertainty. The incompatible elements Rb, Nb, Th, Ce, Yb, La, Cs, Hf, and U display an increase with increasing values of SiO2, as expected if the lavas are related by fractional crystallization. There is a lot of scatter in the Yb plot. However, a slight increasing

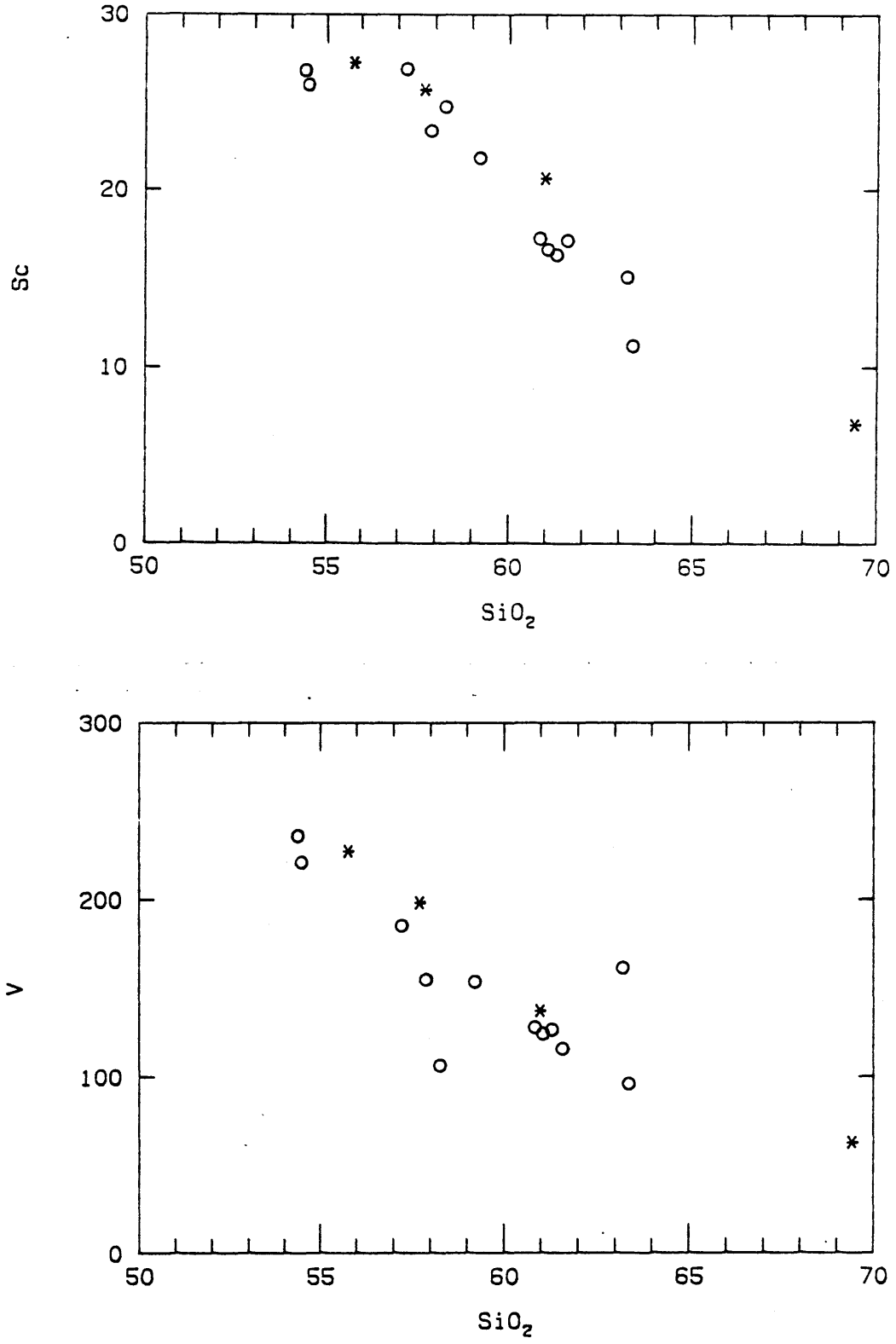

Fig. 4. Variation diagrams for the trace elements vs. SiO2
* - representative sample

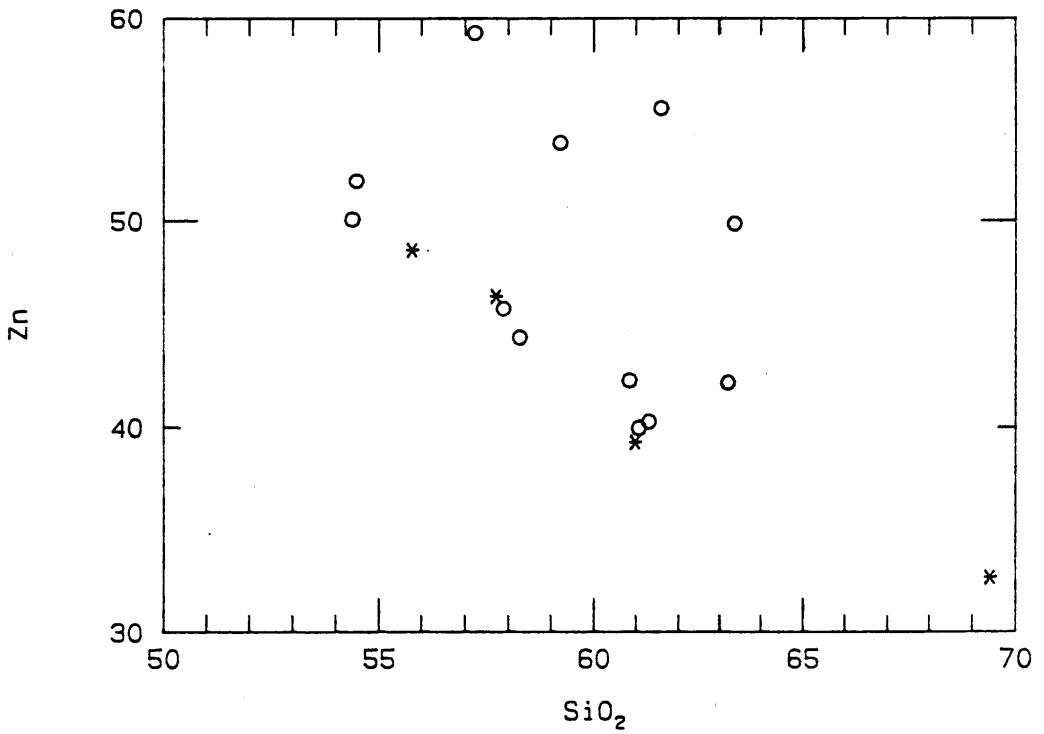
60
50
40
30
Zn
50
55
60
65
70
SiO2

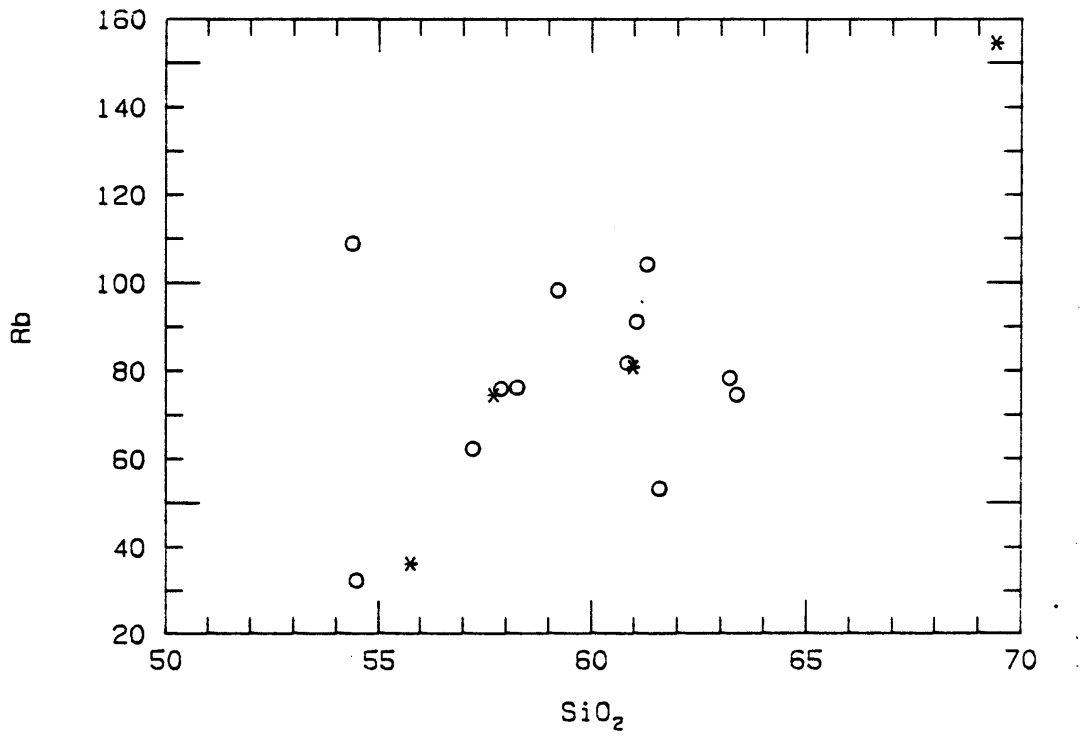
160
140
120
100
80
60
40
20
Rb
50
55
60
65
70
SiO2

Fig. 4. (cont.)

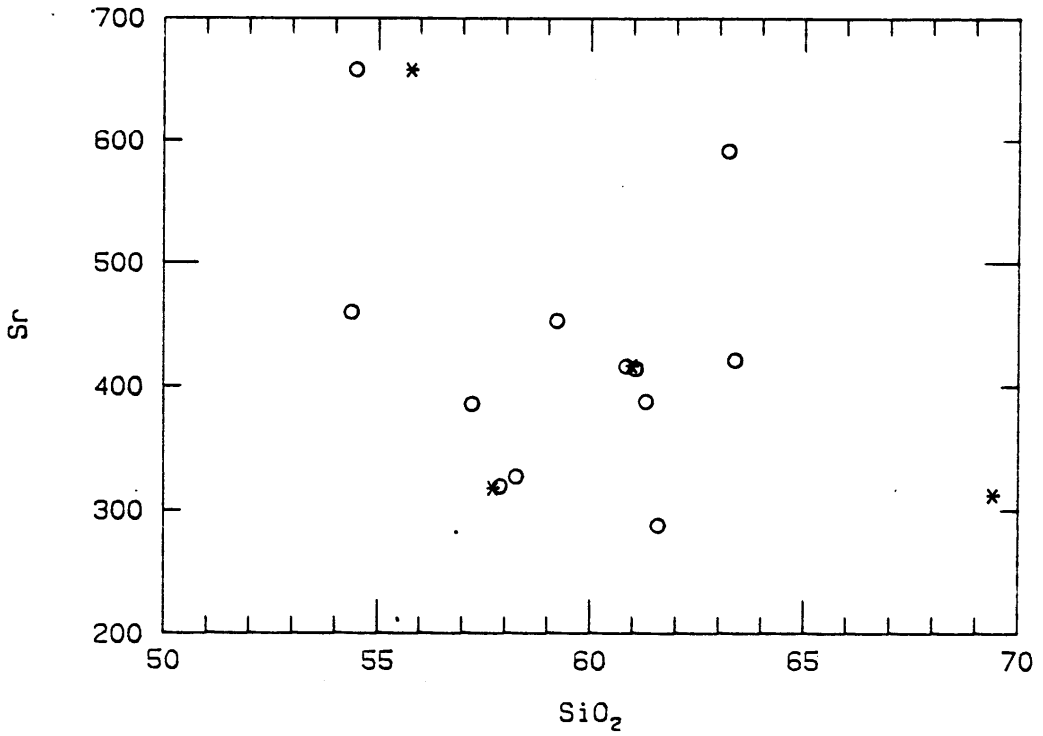
700
600
500
400
300
200
Sr
50
55
60
65
70
SiO2

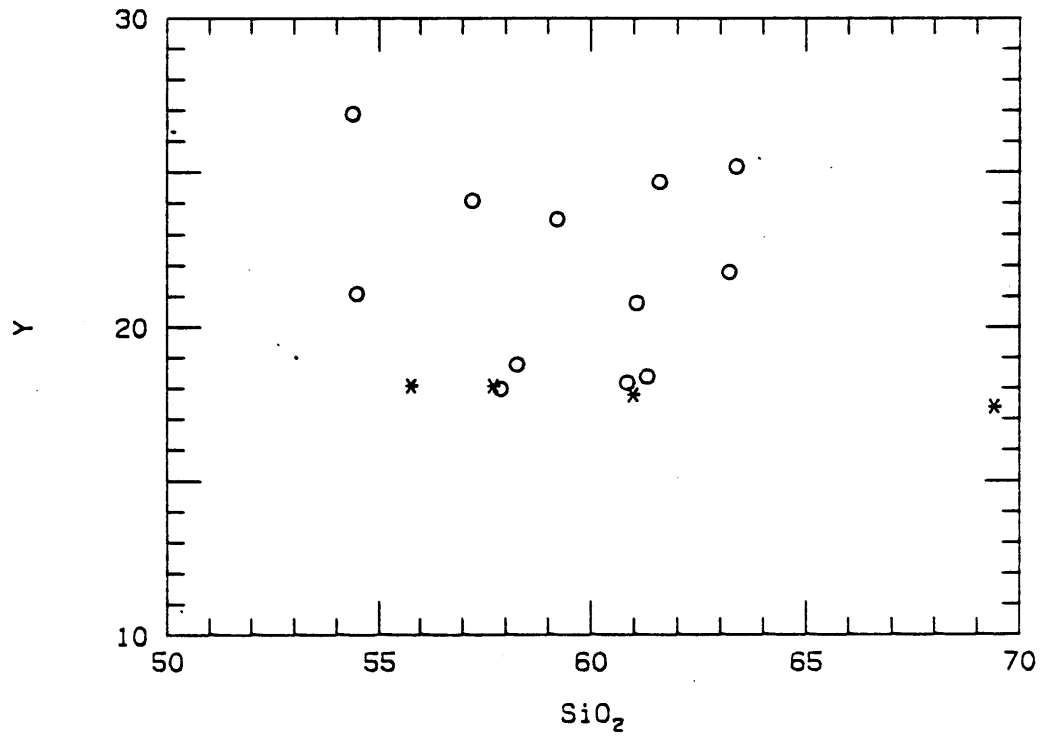
30
20
10
Y
50
55
60
65
70
SiO2

Fig. 4. (cont.)

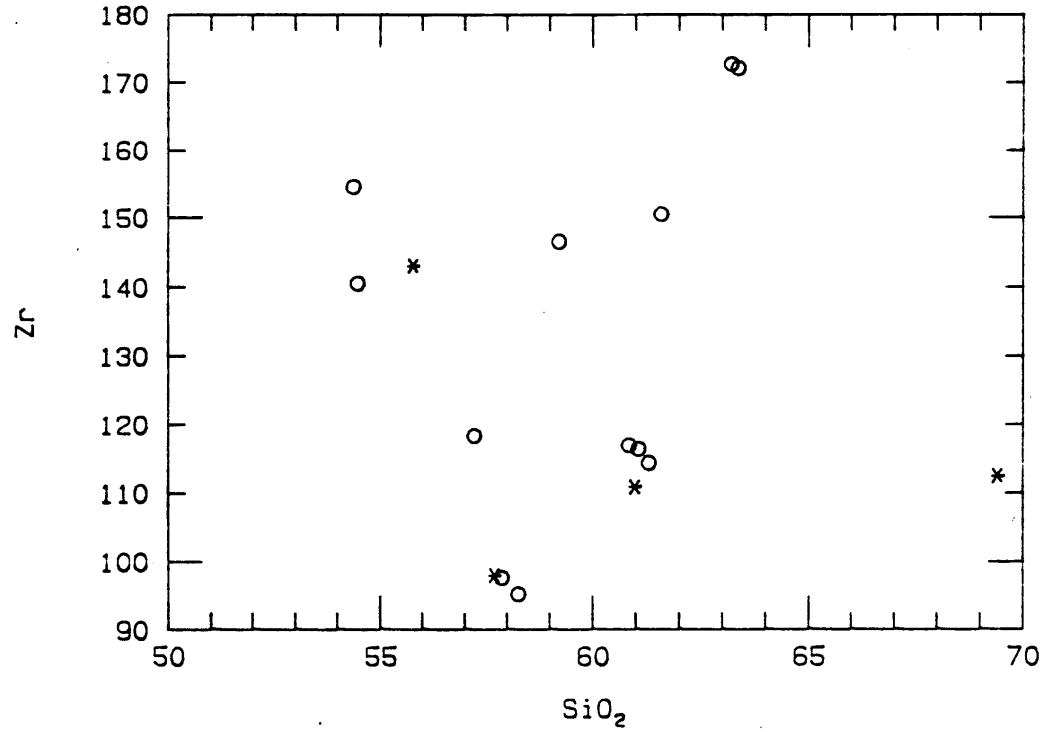
Zr
180
170
160
150
140
130
120
110
100
90
50
55
60
65
70
SiO2

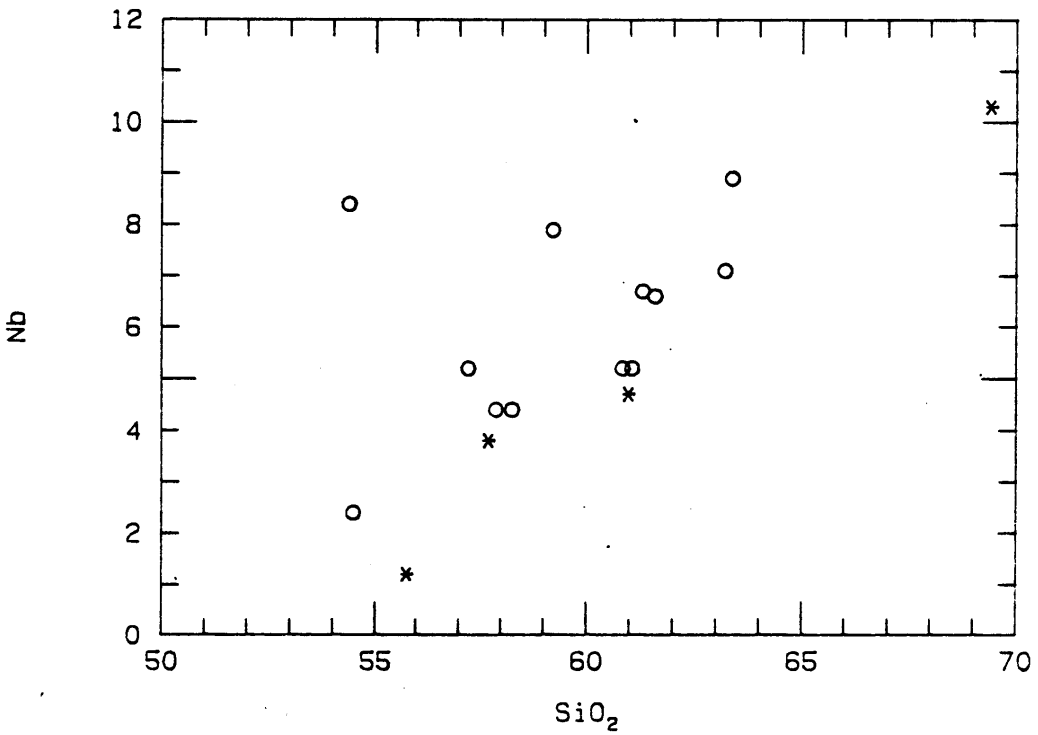
Nb
12
10
8
6
4
2
0
50
55
60
65
70
SiO2

Fig. 4. (cont.)

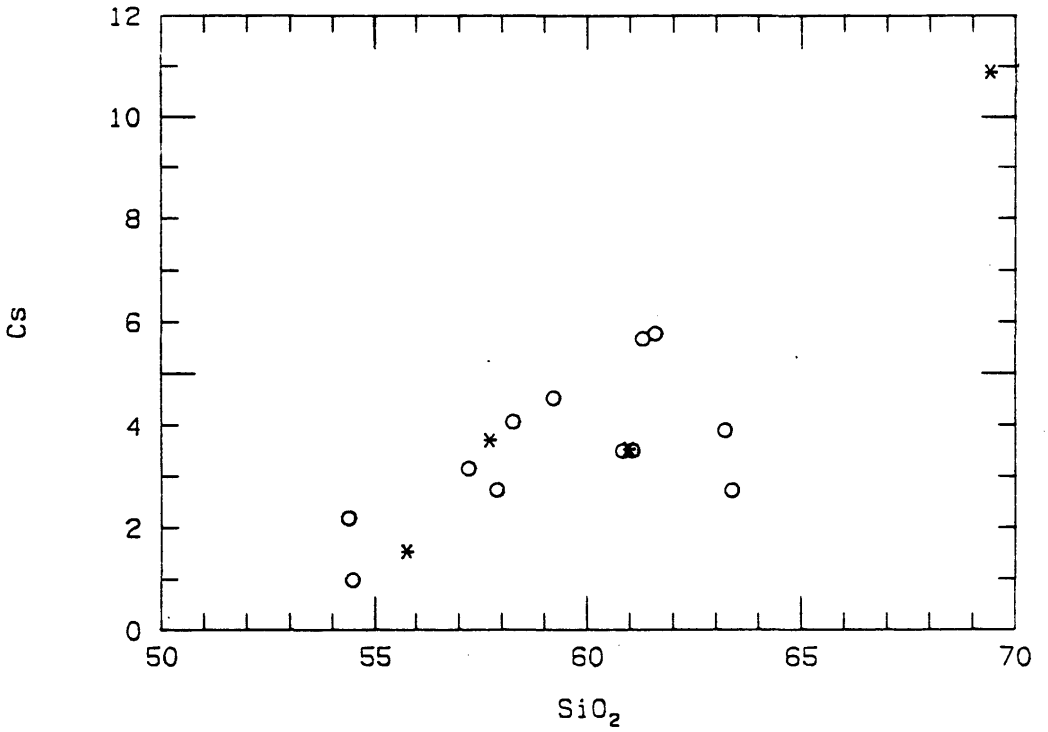

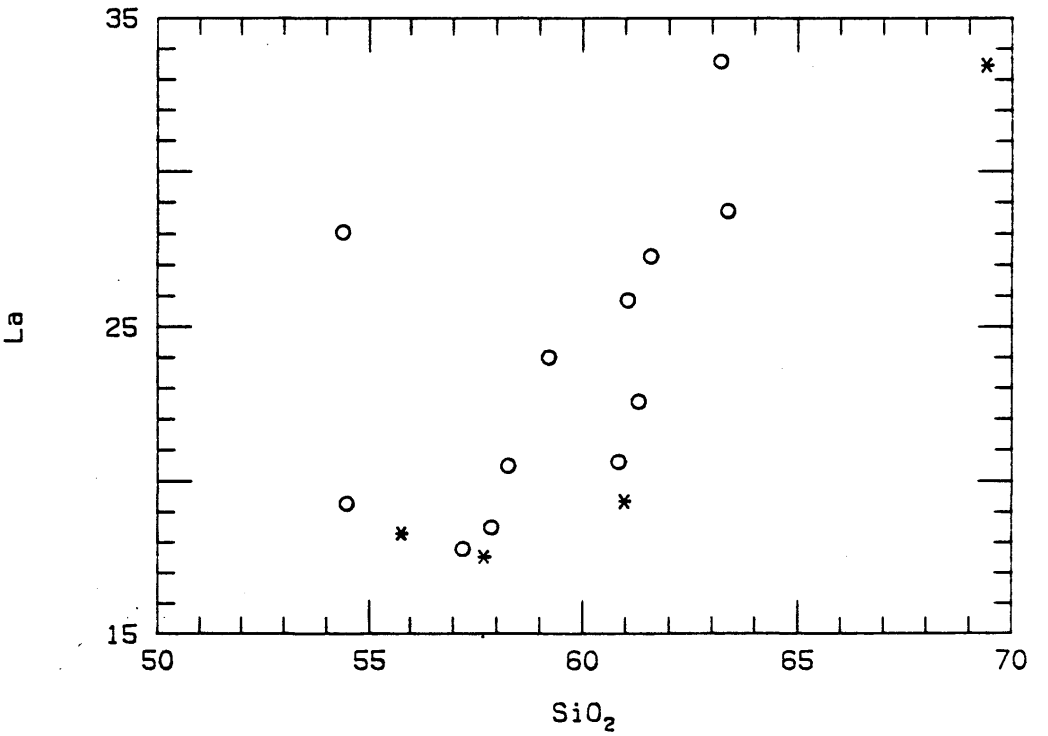

Fig. 4. (cont.)

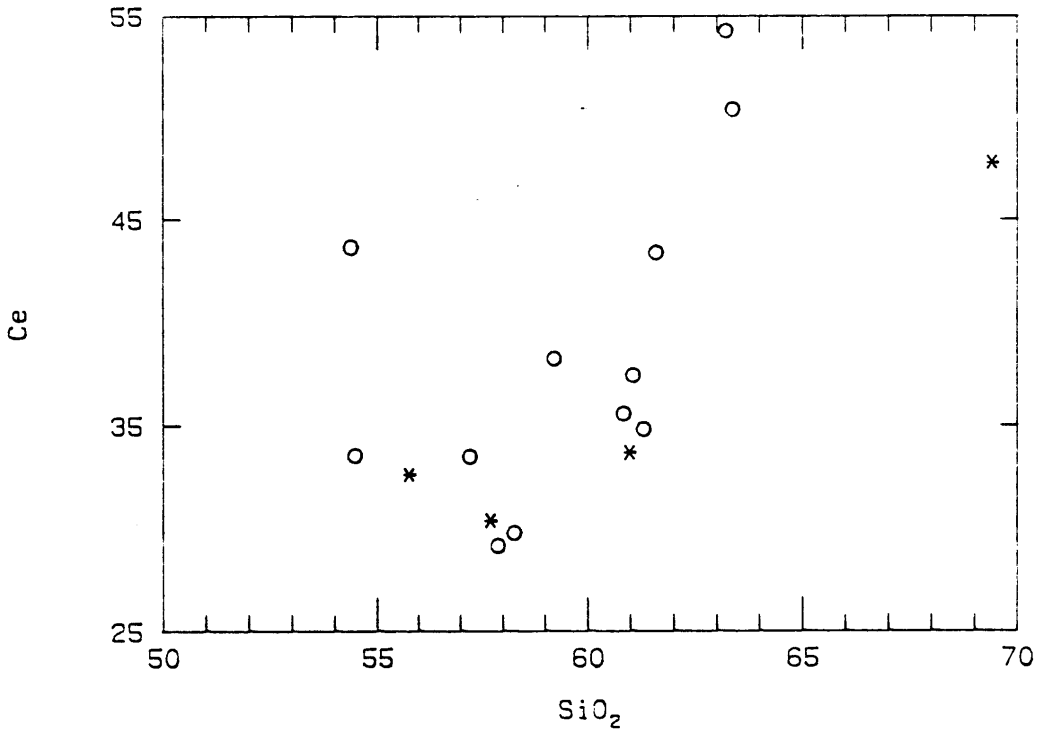

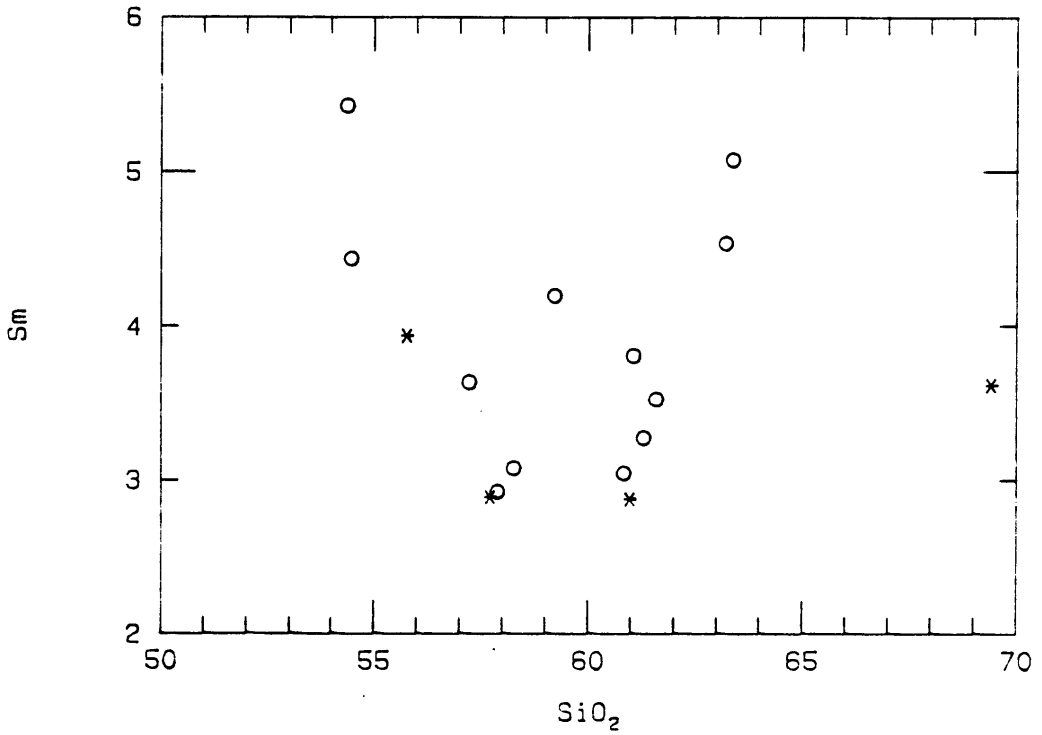

Fig. 4. (cont.)

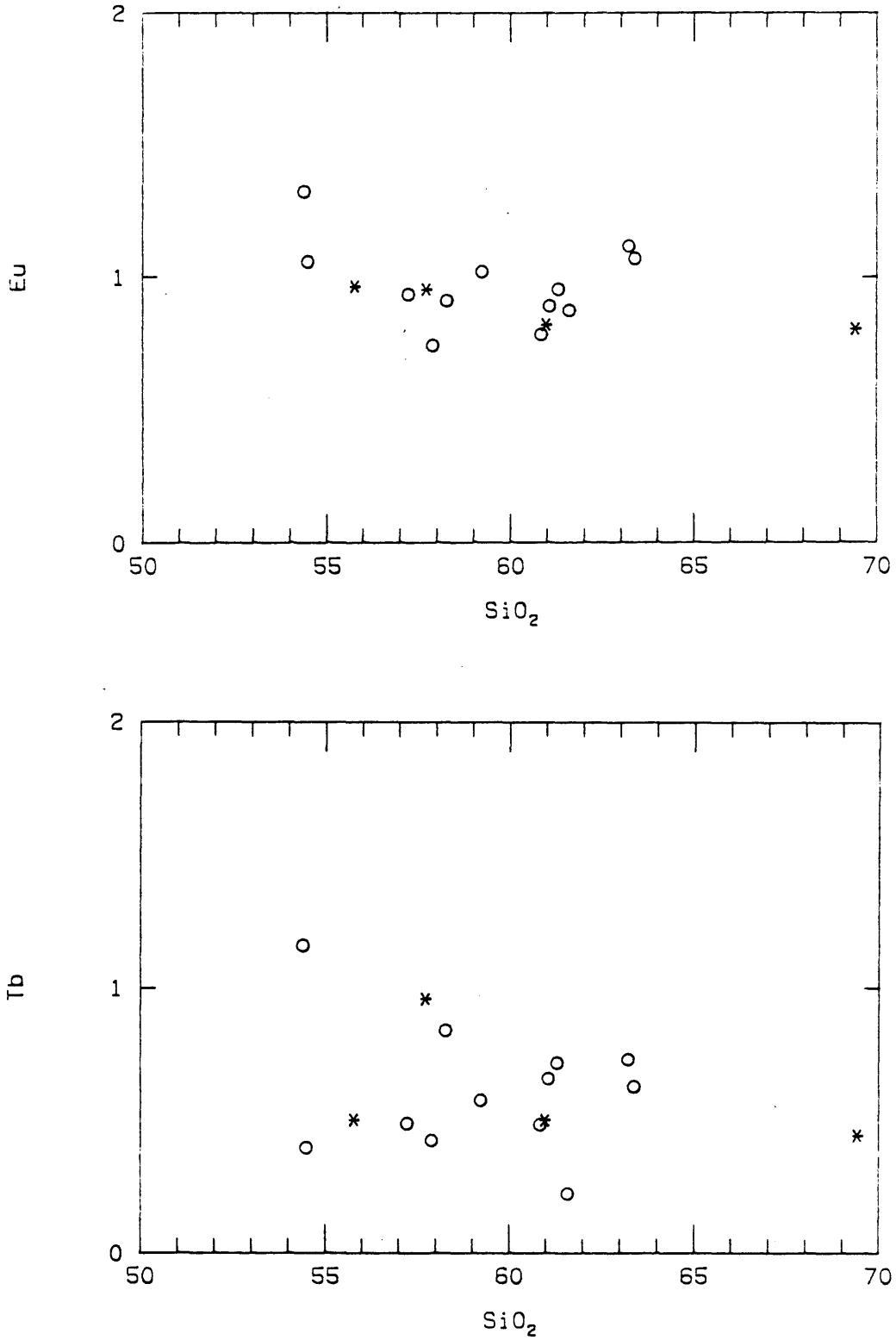

Fig. 4. (cont.)

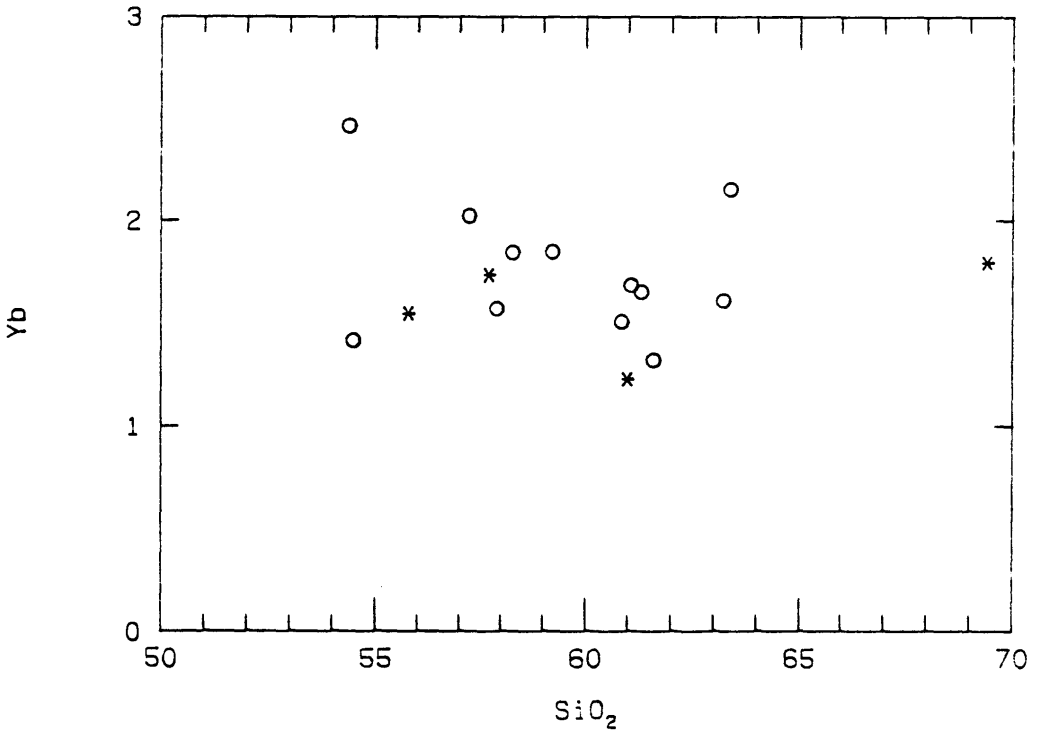

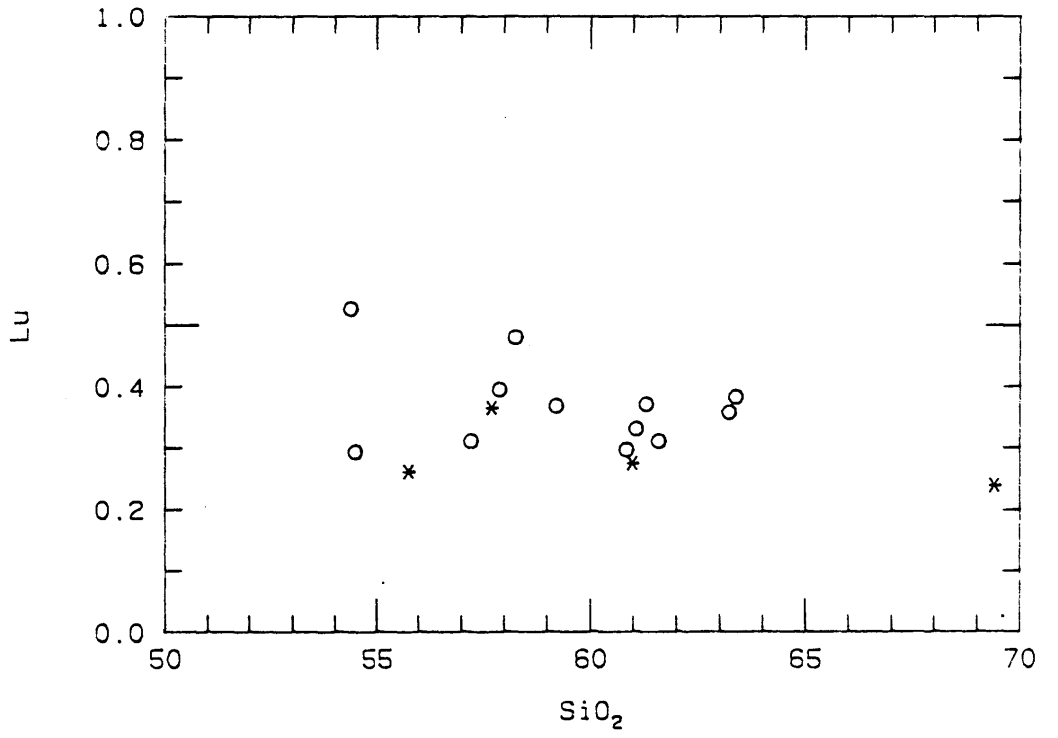

Fig. 4. (cont.)

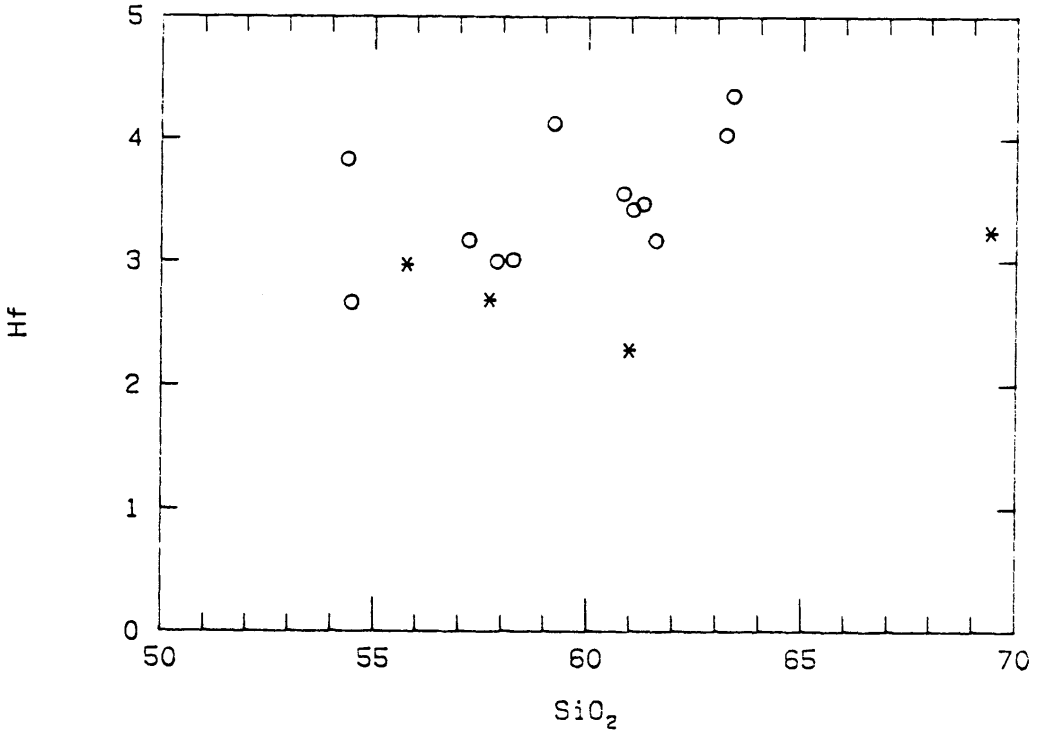

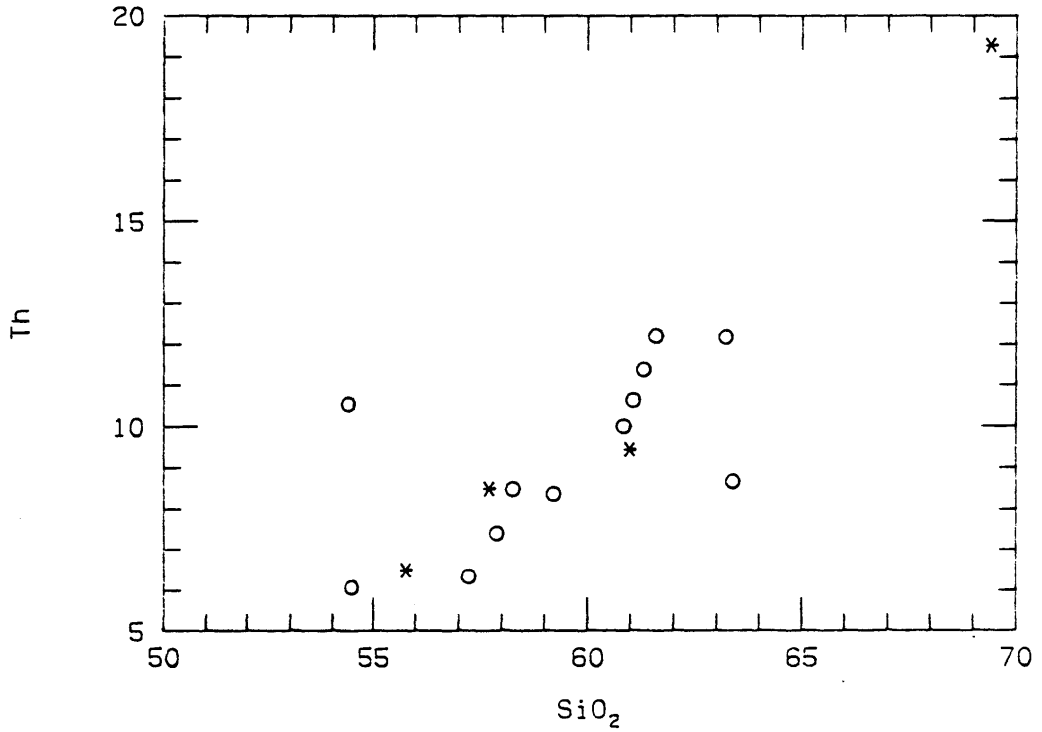

Fig. 4. (cont.)

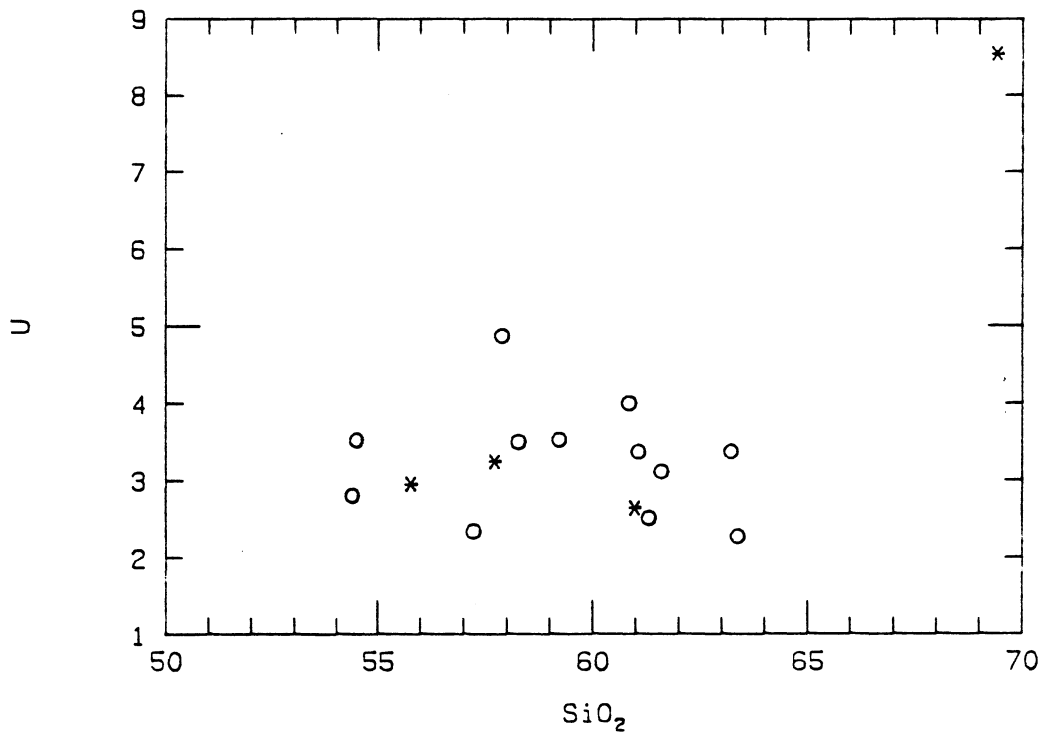

Fig. 4. (cont).

trend is discernable. The plots of Lu and Eu, both Rare Earth Elements, display unexpected trends. These elements are considered incompatibles, yet they decrease slightly with increasing values of SiO2. The decrease in Eu probably reflects the incorporation of Eu in plagioclase throughout the evolution of the magmas. The negative slope for Lu is probably due to apatite fractionation, although fractionation of zircon is a possibility, too (Huijsmans, 1985).

The variations of the compatible elements Sc, V, Zn, and Sr all show negative slopes against SiO2. The slopes for Sc, V, and Zn probably result from the fractionation of clinopyroxene and magnetite, and that of Sr is due to its

incorporation in plagioclase.

In order to understand the behavior of these elements, it is helpful to look at their distribution coefficients (D). These are simply expressions of predicting how readily an element enters the structure of a crystallizing phase. Those elements with D>1 are termed compatible, meaning they are preferentially incorporated into a crystal structure. If follows, then, that those elements with D<1 are incompatible and thus, concentrated in the liquid. The bulk distribution coefficients of the elements in each differentiation step were calculated from the Rayleigh distillation equation:

$$C/Co = F^{D-1}$$

where D is the bulk distribution coefficient, C is the concentration of the element in the daughter magma, Co is the concentration in the parent magma, and F is the fraction of liquid remaining (relative to 1.0). The results of this calculation are listed in Table III. Those of Ta, Ba, and Cr will be ignored due to analytical uncertainty. The values for Eu and Lu largely parallel their trends in the variation diagrams in Fig. 4.

Perhaps the most important feature to note is the large number of negative values for D, especially in the initial step. Looking at the graph in Fig. 5, it is apparent that fractional crystallization alone cannot produce

Table III. Distribution Coefficients of the Trace Elements (R=concentration in daughter magma, Ro=concentration in parent magma)

Aeg 3 - Aeg 14

Elem	R	Ro	D
Sc	25.7600	27.2900	1.5160
V	198.4900	227.3900	2.2155
Cr	143.8900	30.4500	-12.8873
Zn	46.4000	48.6000	1.4143
Rb	74.6000	36.3000	-5.4415
Sr	318.2000	658.0000	7.4969
Y	18.1000	18.1000	1.0000
Zr	98.0000	143.1000	4.3854
Nb	3.8000	1.2000	-9.3078
Cs	3.7100	1.5400	-6.8627
Ba	467.0000	296.0000	-3.0775
La	17.5400	18.3100	1.3842
Ce	30.4100	32.6400	1.6328
Sm	2.8940	3.9400	3.7591
Eu	0.9550	0.9660	1.1024
Tb	0.9600	0.5050	-4.7444
Yb	1.7400	1.5500	-0.0340
Lu	0.3660	0.2620	-1.9894
Hf	2.6900	2.9750	1.9005
Th	8.5000	6.5100	-1.3052
U	3.2500	2.9600	0.1642

f
0.8942

Aeg 14 - Aeg 13

Elem	R	Ro	D
Sc	20.7000	25.7600	2.0330
V	137.2900	198.4900	2.7413
Cr	88.1000	143.8900	3.3172
Zn	39.3000	46.4000	1.7844
Rb	81.0000	74.6000	0.6112
Sr	417.2000	318.2000	-0.2795
Y	17.8000	18.1000	1.0789
Zr	110.9000	98.0000	0.4159
Nb	4.7000	3.8000	-0.0040
Cs	3.5400	3.7100	1.2216
Ba	684.0000	467.0000	-0.8026
La	19.3500	17.5400	0.5361
Ce	33.7100	30.4100	0.5134
Sm	2.8800	2.8940	1.0229
Eu	0.8220	0.9550	1.7084
Tb	0.5040	0.9600	4.0436
Yb	1.2300	1.7400	2.6384
Lu	0.2760	0.3660	2.3331
Hf	2.2900	2.6900	1.7604
Th	9.4500	8.5000	0.4996
U	2.6500	3.2500	1.9640

f
0.8092

Aeg 13 - Aeg 17

Elem	R	Ro	D
Sc	6.8320	20.7000	3.3820
V	62.4200	137.2900	2.6937
Zn	32.7000	39.3000	1.3951
Rb	154.6000	81.0000	-0.3890
Sr	312.8000	417.2000	1.6189
Y	17.4000	17.8000	1.0488
Zr	112.5000	110.9000	0.9692
Nb	10.3000	4.7000	-0.6859
Cs	10.8900	3.5400	-1.4147
Ba	592.0000	684.0000	1.3104
La	33.4800	19.3500	-0.1781
Ce	47.8300	33.7100	0.2482
Sm	3.6200	2.9800	0.5086
Eu	0.8050	0.8220	1.0449
Tb	0.4460	0.5040	1.2627
Yb	1.8020	1.2300	0.1794
Lu	0.2400	0.2760	1.3003
Hf	3.2360	2.2900	0.2570
Th	19.2900	9.4500	-0.5333
U	8.5500	2.6500	-1.5171

f
0.6279

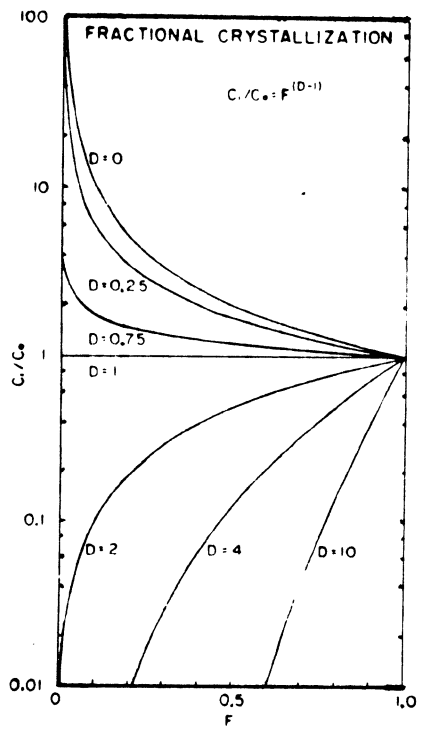

Fig. 5. C/Co vs. F for Rayleigh fractionation law.

values of less than zero. These negative values lie in the area suitably termed the "forbidden zone", and are the result of processes other than fractional crystallization. Unfortunately, the effects of magma mixing and assimilation look the same when plotted on this

graph (i.e. they tend to result in values of D that lie in the forbidden zone).

However, the author believes that Sr isotope data from these samples lends evidence to the possibility of assimilation. One isotope, 87Sr, is a product of the radioactive decay of 87Rb, which is highly concentrated in the crust, relative to the mantle. Therefore, we would expect an increase in 87Sr/86Sr values if crustal material was assimilated. Note the 87Sr/86Sr variations in Fig. 6. A sharp

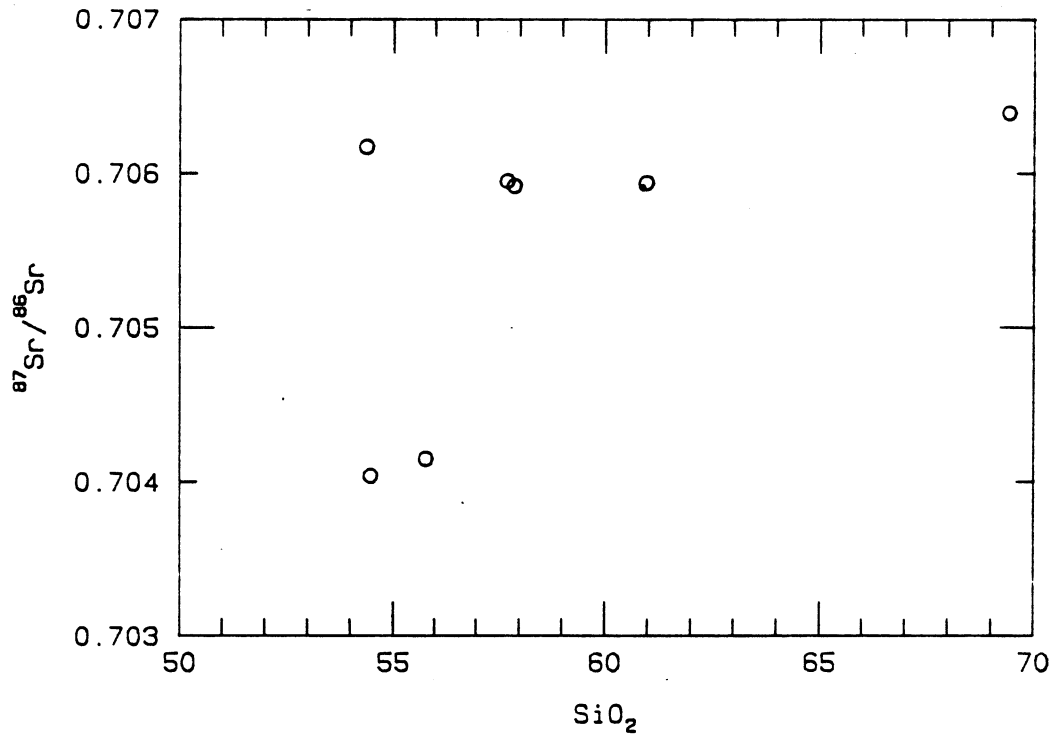

Fig. 6. 87Sr/86Sr variations plotted against SiO2.

increase in the 87Sr/86Sr ratio is seen when SiO2 contents are between 55 and 60 wt. percent, or during the initial differentiation steps.

Another important feature that should be touched upon is the behavior of the Rare Earth Elements. This can be

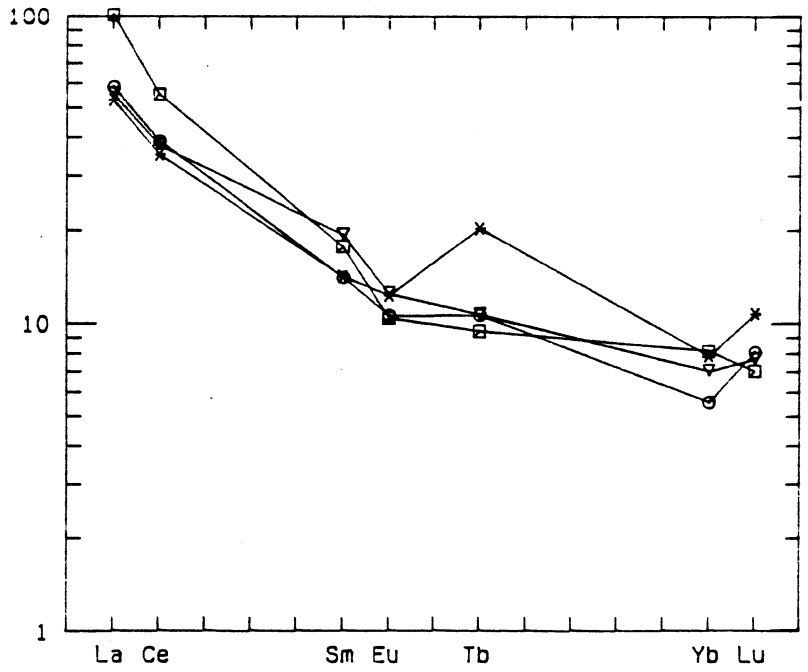

Fig. 7. Chondrite-normalized REE patterns. (triangle= Aeg 3, asterisk=Aeg 14, circle=Aeg 13, square=Aeg 17)

expressed graphically in the chondrite-normalized REE patterns in Fig. 7. All four samples exhibit Light Rare Earth Element (LREE) enrichment, characteristic of calc-alkaline rocks, and slight negative Eu-anomalies, reflecting plagioclase fractionation. The absolute scale of the Eu-anomalies cannot be determined precisely due to the lack of Gd analyses. The high Tb peak for Aeg 14 is due to analytical errors (Barton, pers. comm.). Notice the behavior of the LREE for Aeg 3 and Aeg 14. Aeg 3 displays a slightly greater enrichment in La, Ce, and Sm than Aeg 14. This cannot be due to fractional crystallization alone, but may be the result of some strange type of assimilation (Barton, pers. comm.), though it is not clearly understood at this

time. A similar problem is seen in the Heavy Rare Earth Elements (i.e. Yb and Lu) behavior.

Using widely accepted values of Sr(ppm) and 87Sr/86Sr for the crust, a model was constructed to predict the effects of combined assimilation and fractional crystallization (AFC). The results are presented in Table IV. The

Table IV. Results of AFC modelling.

Aeg 3 - Aeg 13
contaminant - ave. crust
F = 0.8760
r = 0.77
D-Sr = 1.65
87Sr/86Sr (crust) = 0.710
Sr (crust) = 400 ppm

	Cmin	Cmax	Aeg 13
Sc	10.25	37.77	20.70
V	13.36	188.64	137.29
Cr	0.36	49.07	88.10
Zn	5.84	40.66	39.3
Rb	57.34	61.05	81.0
Sr	411.69	411.69	417.2
Zr	182.73	206.47	110.9
Cs	2.56	2.56	3.54
Ba	402.70	498.92	684.0
La	-	-	19.35
Ce	46.08	54.47	33.71
Sm	4.80	6.13	2.88
Eu	0.96	1.58	0.822
Yb	2.16	2.77	1.23
Hf	4.16	4.68	2.29
Th	8.95	9.66	9.450

Aeg 3 - Aeg 13
contaminant - ave. crust
F = 0.6720
r = 0.54
D-Sr = 1.41
87Sr/86Sr (crust) = 0.710
Sr (crust) = 400 ppm

	Cmin	Cmax	Aeg 13
Sc	7.01	43.74	20.70
V	9.24	179.03	137.29
Cr	0.25	55.37	88.10
Zn	2.47	45.35	39.3
Rb	70.44	77.51	81.0
Sr	416.86	416.86	417.2
Zr	217.67	261.97	110.9
Cs	3.27	3.27	3.54
Ba	456.07	631.64	684.0
La	32.14	35.39	19.35
Ce	53.34	68.80	33.71
Sm	5.35	7.75	2.88
Eu	0.94	1.98	0.822
Yb	2.39	3.49	1.23
Hf	4.92	5.88	2.29
Th	10.99	12.34	9.450

Aeg 3 - Aeg 13
contaminant - upper crust
F = 0.6720
r = 0.54
D-Sr = 1.41
87Sr/86Sr (crust) = 0.710
Sr (crust) = 350 ppm

	Cmin	Cmax	Aeg 13
Sc	3.69	34.07	20.70
V	3.19	139.54	137.29
Zn	10.19	68.80	39.3
Rb	106.99	116.29	81.0
Sr	400.94	400.94	417.0
Zr	288.35	340.72	110.9
Ba	618.68	830.34	684.0
La	37.82	41.41	19.35
Ce	65.90	83.50	33.71
Sm	5.71	8.20	2.88
Eu	0.87	1.86	0.822
Yb	2.39	3.49	1.23
Hf	6.32	7.44	2.29
Th	14.03	15.59	9.450

Aeg 3 - Aeg 13
contaminant - lower crust
F = 0.6720
r = 0.54
D-Sr = 1.41
87Sr/86Sr (crust) = 0.710
Sr (crust) = 425 ppm

	Cmin	Cmax	Aeg 13
Sc	8.67	48.57	20.70
V	12.14	197.92	137.29
Rb	52.16	58.12	81.0
Sr	424.82	424.82	417.2
Zr	182.33	222.59	110.9
Ba	574.76	532.28	684.0
La	29.56	32.65	19.35
Ce	47.05	61.46	33.71
Sm	5.16	7.52	2.88
Eu	0.98	2.03	0.822
Yb	2.39	3.49	1.23
Hf	4.22	5.10	2.29
Th	9.48	10.72	9.450

goal of this model was to obtain trace element values between those of Cmin and Cmax (representing the range of acceptable values for each element), thereby yielding information as to the type of crustal material assimilated. As can be seen from the results, values of Sr for different types of crust were used (i.e. lower, upper, and average crust) for this model. Few of the elements fall within the accepted range of concentrations, the REEs (i.e. La, Ce, Sm, Eu, and Yb) being the most consistant misfits. Previous failures, including this study, to correlate 87Sr/86Sr and trace element values for the AFC model suggest that perhaps the 87Sr/86Sr and Sr(ppm) values for assimilated crustal material may be inaccurate (Barton, pers. comm.). The process of magma mixing may also be responsible for these anomalous results.

However, mixing is believed to have had little or no consequence in the evolution of these magmas (Barton, pers. comm.). There is no definitive evidence for the workings of mixing. For example, if two magmas of differing compositions are mixed, one would expect to find two different compositions of crystallizing phases, most notably plagioclase. Yet, there is no evidence of this in the petrographic analyses. Nevertheless, more detailed studies need to be conducted to concretely refute the role of magma mixing as a mechanism of differentiation.

6.0 CONCLUSIONS AND IMPLICATIONS

The study of differentiation mechanisms on the island of Aegina, in the Aegean Sea, indicates the following:

1.) The compositional range, basaltic andesite to rhyodacite is due largely to differentiation by fractional crystallization.
2.) Petrographic studies fail to give evidence of magma mixing.
3.) The results of the least-squares mixing model, likewise, indicates the probability of fractional crystallization.
4.) Anomalous trace element behavior (D<0) and REE patterns cannot be explained by fractional crystallization alone, but by the additional workings of other processes.
5.) 87Sr/86Sr variations indicate assimilation of crustal material accompanying fractional crystallization during the early stages of magma evolution.
6.) Failure of the AFC model suggests the use of inaccurate values of Sr(ppm) and 87Sr/86Sr for assimilated crust.

The results from the major and trace element and iso-

topic studies presented closely parallel the conclusions of Till (1986):

1.) Fractional crystallization acted continuously throughout the evolution of the magma body.

2.) Fractional crystallization was accompanied by assimilation in the early stages of differentiation, most probably in the lower crust. The magma body would have to expend less energy assimilating hotter material from the lower crust than it would in incorporating cooler material from other parts of the crust.

ACKNOWLEDGEMENTS

I would like to thank Dr. Michael Barton for his patient guidance and for the use of all data. My thanks also to Dennis Schucker and Rodney Sheets for their computer expertise, and to Joyce (Alex) Riter, Jeff Swope, and Michael Barton for their unselfish lending of various literature.

REFERENCES

Barton, M., Salters, V.J.M., and Huijsmans, J.P.P. (1983). Sr isotope and trace element evidence for the role of continental crust in calc-alkaline volcanism on Santorini and Milos, Aegean Sea, Greece. Earth Planet Sci. Lett. 63:273-291.

Barton, M., and Huijsmans, J.P.P. (1986). Post-caldera dacites from the Santorini volcanic complex, Aegean Sea, Greece: an example of the eruption of lavas of near-constant composition over a 2,200 year period. Contrib. Mineral. and Petrol. 94:472-495.

Cox, K.G., Bell, J.D., and Pankhurst, R.J., 1979. The Interpretation of Igneous Rocks. George Allen & Unwin (Publishers) Ltd., London, 450 pp.

Fytikas, M., Giuliani, O., Innocenti, F., Marinelli, G., and Mazzuoli, R. (1976). Geochronological data on Recent magmatism of the Aegean Sea. Tectonophysics. 31:T29-T34.

Green, T.H. (1980). Island arc and continent-building magmatism - a review of petrogenic models based on experimental petrology and geochemistry. Tectonophysics. 63:367-385.

Huijsmans, J.P.P., 1985. Calc-alkaline Lavas from the Volcanic Complex of Santorini, Aegean Sea, Greece: A petrological, geochemical, and stratigraphic study. Thesis. State University of Utrecht (The Netherlands)

Hughs, C.J., 1982. Igneous Petrology. Elsevier Scientific Publishing Co., Amsterdam, The Netherlands, 551 pp.

Ringwood, A.E. (1974). Petrological evolution of island arc systems. J. Geol. Soc. London. 130:183-204.

Till, Barbara Sue. (1986). Fractional crystallization calculations based on whole-rock and phenocryst element oxide weight percentages from Aegina, Aegean Sea, Greece. Unpublished undergraduate thesis. The Ohio State University, Columbus, Ohio.

Wyers, G.P. and Barton, M. (1986). Petrology and evolution of transitional alkaline-subalkaline lavas from Patmos, Dodecanesos, Greece: evidence for fractional crystallization, magma mixing, and assimilation. Contrib. Mineral. and Petrol. 93:297-311.